J Korean Med Sci. 2025 Jan 6;40(1):e2
https://doi.org/10.3346/jkms.2025.40.e2
eISSN 1598-6357·pISSN 1011-8934

JKMS

Original Article

Humanities & Basic Medical Science

Check for updates

Artemisinin-Quinidine Combination for Suppressing Ventricular Tachyarrhythmia in an Ex Vivo Model of Brugada Syndrome

Hyung Ki Jeong,[1,2] **Namsik Yoon**,[3,4] **Yoo Ri Kim**,[3,4] **Ki Hong Lee**,[3,4] **and Hyung Wook Park**[3,4]

[1]Division of Cardiology, Department of Internal Medicine, Wonkwang University School of Medicine, Iksan, Korea
[2]Institute of Wonkang Medical Science, Iksan, Korea
[3]Division of Cardiology, Department of Internal Medicine, Chonnam National University Medical School, Gwangju, Korea
[4]Department of Cardiovascular Medicine, Chonnam National University Hospital, Gwangju, Korea

OPEN ACCESS

Received: Jul 4, 2024
Accepted: Sep 12, 2024
Published online: Oct 18, 2024

Address for Correspondence:
Namsik Yoon, MD, PhD
Division of Cardiology, Department of Internal Medicine, Chonnam National University Medical School; Department of Cardiovascular Medicine, Chonnam National University Hospital, 42 Jaebong-ro, Dong-gu, Gwangju 61469, Republic of Korea.
Email: yoonnamsik@gmail.com

ORCID iDs
Hyung Ki Jeong
https://orcid.org/0000-0001-5749-9525
Namsik Yoon
https://orcid.org/0000-0001-9112-150X
Yoo Ri Kim
https://orcid.org/0000-0001-7351-1299
Ki Hong Lee
https://orcid.org/0000-0002-9938-3464
Hyung Wook Park
https://orcid.org/0000-0002-9630-0467

ABSTRACT

Background: The ionic mechanism underlying Brugada syndrome (BrS) arises from an imbalance in transient outward current flow between the epicardium and endocardium. Previous studies report that artemisinin, originally derived from a Chinese herb for antimalarial use, inhibits the Ito current in canines. In a prior study, we showed the antiarrhythmic effects of artemisinin in BrS wedge preparation models. However, quinidine remains a well-established antiarrhythmic agent for treating BrS. Therefore, this study aims to investigate the efficacy of combining artemisinin with low-dose quinidine in suppressing ventricular tachyarrhythmia (VTA) in experimental canine BrS models.
Methods: Transmural pseudo-electrocardiogram and epicardial/endocardial action potential (AP) were recorded from coronary-perfused canine right ventricular wedge preparation. To mimic the BrS model, acetylcholine (3 μM), calcium channel blocker verapamil (1 μM), and Ito agonist NS5806 (6–10 μM) were administered until VTA was induced. Subsequently, low-dose quinidine (1–2 μM) combined with artemisinin (100 μM) was perfused to mitigate VTA. Key parameters, including AP duration, J wave area, notch index, and T wave dispersion, were measured.
Results: After administering the provocation agents, all sample models exhibited prominent J waves and VTA. Artemisinin alone (100–150 μM) suppressed VTA and restored the AP dome in all three preparations. Its infusion resulted in reductions in the J wave area and epicardial notch index. Consequently, low-dose quinidine (1–2 μM) did not fully restore the AP dome in all six sample models. However, when combined with additional artemisinin (100 μM), low-dose quinidine effectively suppressed VTA in all six models and restored the AP dome while also decreasing the J wave area and epicardial notch index.
Conclusion: Low-dose quinidine alone fails to fully alleviate VTA in the BrS wedge model. However, its combination with artemisinin effectively suppresses VTA. Artemisinin may reduce the therapeutic dose of quinidine, potentially minimizing its associated adverse effects.

Keywords: Brugada Syndrome; Anti-Arrhythmia Agents; Sudden Cardiac Death; Quinidine; Artemisinin

Funding

This study was supported by a National Research Foundation of Korea grant funded by the Korea government (MSIT) (No. RS-2023-00252178).

Disclosure

The authors have no potential conflicts of interest to disclose.

Author Contributions

Conceptualization: Jeong HK, Kim YR, Lee KH, Park HW, Yoon N. Data curation: Jeong HK, Yoon N. Formal analysis: Jeong HK, Yoon N. Funding acquisition: Yoon N. Investigation: Jeong HK, Kim YR, Lee KH, Park HW, Yoon N. Methodology: Yoon N. Project administration: Yoon N. Resources: Yoon N. Software: Jeong HK. Supervision: Yoon N. Validation: Yoon N. Visualization: Jeong HK. Writing - original draft: Jeong HK. Writing - review & editing: Kim YR, Lee KH, Park HW, Yoon N.

INTRODUCTION

Brugada syndrome (BrS) manifests as sudden cardiac death (SCD) and is associated with fatal ventricular tachyarrhythmia (VTA) without evident macro-structural heart disease.[1,2]

Two theories explain the mechanisms of BrS centers: depolarization and repolarization.[3,4] The depolarization theory attributes the characteristic BrS electrocardiogram (ECG) to slow conduction, owing to factors such as fibrosis and reduced Cx43 in the right ventricle (RV) and right ventricular outflow tract (RVOT).[5-7] In contrast, the repolarization theory suggests that a transmural voltage gradient between the epicardium and endocardium—caused by decreased inward currents (INa, ICa) and unopposed outward currents (Ito, IK-ATP)—underlies BrS. Genetic mutations can exacerbate these imbalances, leading to phase 2 reentry and VTA. Studies on canine models show that altering these electrical currents can trigger the BrS ECG phenotype and VTA.[8-12] A recent study by Behr et al.[3] highlights the role of depolarization and repolarization mechanisms in the underlying pathogenesis of BrS.

The implantable cardioverter defibrillator (ICD) is the only proven treatment for preventing SCD in patients with BrS.[13,14] However, lead-related complications such as infection and lead failure are particularly concerning given the relatively young age at which SCD occurs in BrS. Lead durability is a critical issue, with studies reporting a 29% ICD lead failure rate in patients with BrS during follow-up.[15,16] Additionally, frequent shocks owing to VTA affect the quality of life. Therefore, pharmacological treatments are necessary for primary or secondary prevention of fatal VTA in patients with BrS. Decades ago, Ito channel inhibition was identified as a potential medical therapy for BrS. For example, quinidine, an Ito channel inhibitor, is employed during VTA storms in patients with BrS, following current guidelines.[13,14] Although the exact electrophysiological mechanism of quinidine is not fully understood, it acts on sodium and potassium channels, as well as muscarinic receptors, and is categorized as a class IA antiarrhythmic drug. In BrS, the inhibition of quinidine in potassium channels, particularly the Ito channel, plays a crucial role in suppressing VTA. This helps reduce ICD shocks and improve electrical instability in these patients. However, side effects are common, with gastrointestinal symptoms, particularly diarrhea, being the most frequent. Quinidine also carries a proarrhythmic risk, such as QT prolongation, which can potentially result in SCD. Therefore, to mitigate this risk, some studies recommend monitoring plasma levels.[17] The current recommended dose of 900 mg/day to 1.5 g/day could be considered relatively excessive, resulting in significant side effects that many patients find intolerable in the long term.[10,11] Artemisinin, derived from the sweet wormwood plant (Artemisia annua), has been utilized in traditional Chinese medicine to treat fever for over 2000 years.[18] Its pharmacological safety is well-established, as it is widely used for malaria treatment. Beyond its antimalarial properties, artemisinin shows efficacy in inhibiting Ito, IK1, IKr, and IKs channels in a previous canine experimental model.[19,20] Previous studies also show that artemisinin exerts antiarrhythmic effects in wedge preparation models of BrS.[21] Nevertheless, quinidine remains a potent antiarrhythmic agent for BrS. Therefore, this study aims to investigate the role of artemisinin combined with a low dose of quinidine in suppressing VTA in a canine experimental BrS model.

METHODS

Wedge preparations and electrogram recordings

The methods for arterially perfused ventricular wedge preparation and recording of the transmembrane action potential (AP) were employed as previously described.[22,23] Adult mongrel dogs weighing 25–30 kg were obtained from Orient Bio, Inc. (Seongnam, Korea). Heparin (1,000 U/kg, intravenous [IV]) was administered for anticoagulation, followed by anesthesia with pentobarbital (30–35 mg/kg, IV). A left thoracotomy was performed to access and explant the heart. Transmural wedge preparations (2.4 × 2.3 × 2.5 cm^3 to 2.2 × 2.0 × 1.7 cm^3) were dissected from the RV-free wall. The marginal branch of the right coronary artery was cannulated, and these preparations were perfused with a cardioplegic solution (Tyrode's containing 12 mmol/L KCL). Subsequently, the preparations were immersed in a tissue bath and perfused with oxygenated Tyrode's solution (containing NaCl 129 mM, KCl 4 mM, NaH_2PO_3 20 mM, $CaC1_2$ 1.8 mM, $MgSO_4$ 0.5 mM, and glucose 5.5 mM, pH: 7.4). A roller pump (Masterflex 7518-10; Cole-Parmer Instrument Co., Vernon Hills, IL, USA) was utilized to maintain a consistent flow rate of 8–10 mL/min, with the temperature controlled at 37 ± 0.5°C.

The preparations were allowed to equilibrate until electrical stability was confirmed in the tissue bath. Bipolar silver electrodes that were insulated except at the tips were utilized to stimulate the endocardial surface at a basic cycle length of 1,000 ms. Pseudo-ECG data were recorded transmurally using two AgCl half-cell electrodes located 1–1.5 cm from the endocardial and epicardial surfaces, aligned with the axis of the transmembrane recordings. The epicardial electrode was connected to a positive input of the ECG amplifier (MP150CE; Biopac Systems Inc., Goleta, CA, USA). Floating microelectrodes (DC resistance: 10–20 MΩ), filled with 2.7 mol/L KCl, were employed to simultaneously record transmembrane APs from the epicardial and endocardial sites. The electrodes were then connected to a high-input impedance amplifier (Electro 705 electrometer, FD223-G; World Precision Instruments Inc., Sarasota, FL, USA). Impalements were made at epicardial and endocardial positions corresponding to the transmural axis of the pseudo-ECG recordings (**Fig. 1**). Two wedge preparations were served as time-controls, three for artemisinin alone, two for the full dose of quinidine alone, and six for low-dose quinidine combined with artemisinin (**Table 1**).

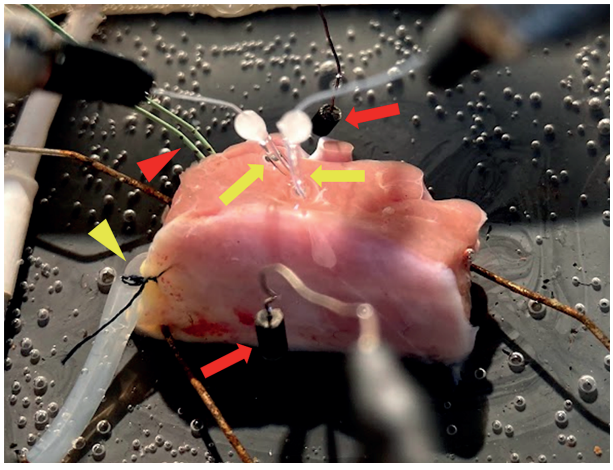

Fig. 1. A right ventricular wedge preparation in a tissue bath. The red arrowhead indicates pacing on the endocardial surface, while the yellow arrows indicate the floating microelectrodes on the Endo and Epi. Two pseudo-ECG leads are placed approximately 1–1.5 cm from the Endo and Epi (red arrowheads). The coronary artery is perfused with oxygenated Tyrode's solution (yellow arrowhead).
ECG = electrocardiogram, Endo = endocardium, Epi = epicardium.

https://doi.org/10.3346/jkms.2025.40.e2

Table 1. Experimental model setups and findings of AP and electrocardiograms

Model No.	Provocation agents, μM			PVT induction	Quinidine, μM	AP dome recovery	PVC recurrence	PVT recurrence	Artemisinin, μM	AP dome recovery	PVC recurrence	PVT recurrence
	NS5806	ACh	Vera									
Artemisinin												
1	7	3	1	+	NA	NA	NA	NA	100	+	–	–
2	6	3	1	+	NA	NA	NA	NA	150	+	–	–
3	6	3	1	+	NA	NA	NA	NA	150	+	+	–
Full-dose quinidine												
4	6	3	1	+	10	+	–	–	NA	NA	NA	NA
5	6	3	1	+	10	+	–	–	NA	NA	NA	NA
Low-dose quinidine + artemisinin												
6	6	3	1	+	1	–	+	+	100	+	–	–
7	6	3	1	+	1	–	+	+	100	+	–	–
8	7	3	1	+	1	–	+	+	100	+	+	–
9	7	3	1	+	2	–	+	–	100	+	–	–
10	7	3	1	+	2	–	+	–	100	+	–	–
11	8	3	1	+	2	–	+	+	100	+	+	–

AP = action potential, ACh = acetylcholine, Vera = verapamil, PVT = polymorphic ventricular tachyarrhythmia (ventricular tachycardia/ventricular fibrillation), PVC = premature ventricular contraction, NA = not applicable.

ECG and AP analysis

Spike 2 software for Windows 10 (Cambridge Electronic Design Ltd., Cambridge, UK) was utilized to record and analyze the ECG, electrograms, and APs.

The onset of the J wave was determined from pseudo-ECG recordings (**Supplementary Fig. 1**). If clearly defined, the onset time is aligned with the notch at the junction between the R and J waves. However, if the demarcation was unclear, the onset time was defined at the point where the negative derivative peaked following the downslope of the R wave. The J wave area was calculated as the product of mV × ms.[12]

In AP recordings, the notch magnitude (calculated as Phase 1 Magnitude/Phase 0 Amplitude × 100) and notch index (Notch Magnitude × [Phase 0 − Phase 2 Interval]), which estimates the notch area, were measured in the epicardium (**Supplementary Fig. 1**).

To calculate the transmural dispersion of repolarization (TDR), the longest interval between the AP durations at 90% of repolarization (APD_{90}) in the endocardium and epicardium was used in simultaneously recorded APs, with adjustments for activation time (AT) differences. The following formula was (**Supplementary Fig. 1**): TDR = (APD_{90} Endocardium + AT Endocardium) + (APD_{90} Epicardium + AT Epicardium).

Evaluation of antiarrhythmic agents

Acetylcholine (3 μM), calcium channel blocker verapamil (1 μM), and Ito channel agonist NS5806 (1-[2,4-dibromo-6-(1H-tetrazol-5-yl)-phenyl]-3-(3,5-bis-trifluoromethyl-phenyl)-urea (Sigma-Aldrich, St Louis, MO, USA) (6–10 μM) were utilized to mimic BrS pharmacologically. The onset of VTA after the infusion of these provocation agents, during stable endocardial stimulation at a basic cycle length of 1,000 ms, was used to define arrhythmia inducibility. To verify the antiarrhythmic effects, artemisinin (C15H22O5; Sigma-Aldrich) (100–150 μM) alone, quinidine (C20H24N2O2; Sigma-Aldrich) (10 μM) alone, and low-dose quinidine (1–2 μM) followed by additional artemisinin (100 μM) were perfused in the BrS models. In previous studies, VTA typically developed spontaneously within 20 minutes following provocation drug administration. Therefore, VTA induction was carefully monitored for up to 40 minutes, and if no VTA occurred by then, the arrhythmia was considered suppressed.

https://doi.org/10.3346/jkms.2025.40.e2

After confirming the antiarrhythmic effect of artemisinin infusion on VTA suppression, the infusion was stopped to observe whether the effect disappeared after the artemisinin washout.

Tissue that exhibited spontaneous ventricular fibrillation/flutter before the BrS phenotype was considered degenerated and then discarded.

Statistical analysis

Data were presented as mean ± standard error of the mean. Continuous variables were compared using the student's *t* test and Mann-Whitney rank-sum test, as appropriate. The Wilcoxon signed-rank test was used to evaluate the effects of artemisinin, quinidine, and their combination. Statistical significance was set at a two-sided *P* value < 0.05. All statistical analyses were performed using IBM SPSS version 27.0 (IBM Corp., Armonk, NY, USA).

Ethics statement

All experiments were conducted in accordance with the Guide for Care and Use of Laboratory Animals Care and Use Committee. The study was approved by the Animal Care and Use Committee at Chonnam National University, Gwangju, Republic of Korea (CNU IACUC-20044).

RESULTS

Time control

Electrograms were recorded from the time-control models (n = 2). Small notches in the epicardial APs and small J waves in pseudo-ECG were observed initially. Even after 6 hours, the wedge preparations remained viable, showing persistently small epicardial notches and J waves (**Supplementary Fig. 2**).

Arrhythmia induction

Figs. 2–5. depicts APs and pseudo-ECG recordings recorded from RV coronary-perfused wedge preparations. Under baseline conditions, a small J wave was observed (**Table 2**). When acetylcholine (3 μM), calcium channel blocker verapamil (1 μM), and Ito channel agonist NS5806 (6–10 μM) were added to the coronary perfusate, the AP notch was enhanced (blue arrowhead in **Fig. 2**), predominantly in the epicardium, with little effect in the endocardium. This also accentuated the J wave (black arrowhead in **Fig. 2**) and caused ST-segment elevation in the pseudo-ECG, mimicking the BrS phenotype. Prolonged exposure caused all-or-none repolarization at the end of the epicardial AP, resulting in the loss of the epicardial AP dome (red arrowhead in **Fig. 2**) in all preparations, ultimately inducing polymorphic ventricular tachycardia (PVT) (**Fig. 2C** column).

Arrhythmogenesis-suppressing effects of artemisinin

After perfusing acetylcholine (3 μM), the calcium channel blocker verapamil (1 μM), and Ito channel agonist NS5806 (6–10 μM), artemisinin (100–150 μM) was incorporated into the coronary perfusate upon phase 2 reentry and VTA development. This finding aligns with that of our previous study,[21] which demonstrates that artemisinin restores the AP dome and decreases repolarization heterogeneity (**Tables 1** and **2**). In two preparations (models 1 and 2 in **Table 1**), neither premature ventricular contractions (PVCs) nor VTA was observed after artemisinin perfusion. In the third preparation (model 3 in **Table 1**), no VTA was induced after the final artemisinin dose, although PVCs were present. Artemisinin

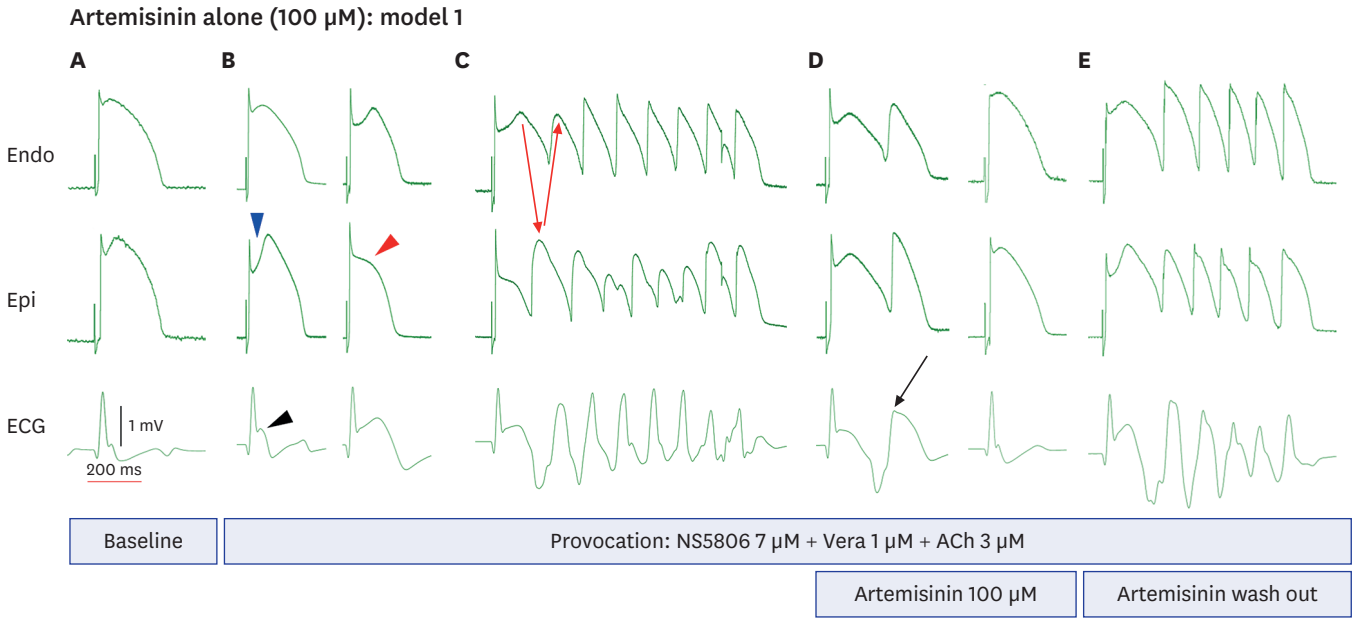

Fig. 2. AP and ECG findings of artemisinin alone (100 μM) in model 1. (**A**) Baseline AP. (**B**) Provocation agents (NS5806, Vera, and ACh) induce BrS phenotypes. After perfusion with artemisinin, Epi AP notching becomes prominent (blue arrowhead), and the J wave is augmented (black arrowhead). The provocation agents induce a loss of dome (red arrowhead). (**C**) PVT is eventually induced through a phase 2 reentry (red arrows). (**D**) Following artemisinin administration, the Epi AP dome is restored, and the J wave decreases, but PVC is still detected (black arrow). Finally, artemisinin offsets the effects of the provocation agents. (**E**) After washing out artemisinin, VTA is induced again.
Endo = endocardium, Epi = epicardium, ECG = electrocardiogram, Vera = verapamil, ACh = acetylcholine, AP = action potential, BrS = Brugada syndrome, PVT = polymorphic ventricular tachycardia, PVC = premature ventricular contraction, VTA = ventricular tachyarrhythmia.

Table 2. Action potential parameters

Effect of agent	Endo APD_{90}, ms	Epi APD_{90}, ms	TDR, ms	Notch index[a]	Notch magnitude, % of Ph 0 amplitude	J wave area, mV × ms
Effect of artemisinin (n = 3)						
Baseline	267.49 ± 3.15	246.34 ± 3.68	18.24 ± 0.92	1,018.32 ± 57.72	18.66 ± 0.84	5.27 ± 0.40
Provocation	279.27 ± 3.35*	251.98 ± 3.61	27.29 ± 1.72*	1,920.89 ± 119.53*	23.85 ± 1.16*	20.51 ± 2.49*
+ Artemisinin (100–150 uM)	251.78 ± 7.45*	236.51 ± 8.71	15.27 ± 2.15*	681.35 ± 66.17*	10.27 ± 0.80*	6.05 ± 0.63*
Effect of quinidine (n = 2)						
Baseline	293.70 ± 3.23	269.75 ± 1.93	23.95 ± 1.74	1,374.93 ± 111.92	22.47 ± 0.43	10.93 ± 0.42
Provocation	288.73 ± 4.04	265.15 ± 1.97	23.58 ± 2.58*	2,452.25 ± 114.94*	30.20 ± 1.24*	17.84 ± 0.38*
+ Quinidine 10 uM	277.25 ± 2.60*	258.41 ± 0.90*	18.83 ± 2.11	502.82 ± 36.86*	8.34 ± 0.61*	5.36 ± 1.08*
Effect of low-dose quinidine & artemisinin (n = 6)						
Baseline	271.05 ± 2.64	252.33 ± 2.57	18.72 ± 0.86	995.87 ± 82.85	16.72 ± 1.27	1.28 ± 0.20
Provocation	282.84 ± 1.14*	259.39 ± 1.04*	23.45 ± 0.72*	2,881.60 ± 160.57*	29.36 ± 1.27*	19.68 ± 1.70*
+ Quinidine 1–2 uM	260.77 ± 3.88*	234.07 ± 4.84*	20.89 ± 2.69*	1,993.04 ± 470.14	15.48 ± 3.35*	18.21 ± 4.89
+ Artemisinin 100 uM	249.90 ± 5.42*	238.00 ± 5.23	11.90 ± 1.01*	473.41 ± 116.59*	6.45 ± 1.13*	3.31 ± 0.94*

Endo = endocardium, APD_{90} = action potential durations at 90% of repolarization, Epi = epicardium, TDR = transmural dispersion of repolarization, Ph = phase.
[a]Notch index: Notch Magnitude × (Ph 0 − Ph 2 Interval), approximating the notch area.
*$P < 0.05$.

(100 μM) effectively suppressed VTA and restored the AP dome in model 1. In models 2 and 3, artemisinin (150 μM) also effectively suppressed VTA (**Fig. 3**). However, this effect disappeared after washout (**Fig. 2**).

Arrhythmogenesis-suppressing effects of quinidine

Quinidine, a potent Ito channel inhibitor, inhibits arrhythmogenesis in the BrS wedge preparation model.[12] Overall, two canine models were utilized as control models to verify the pharmacological effect of quinidine. The BrS model was induced using acetylcholine (3 μM),

https://doi.org/10.3346/jkms.2025.40.e2

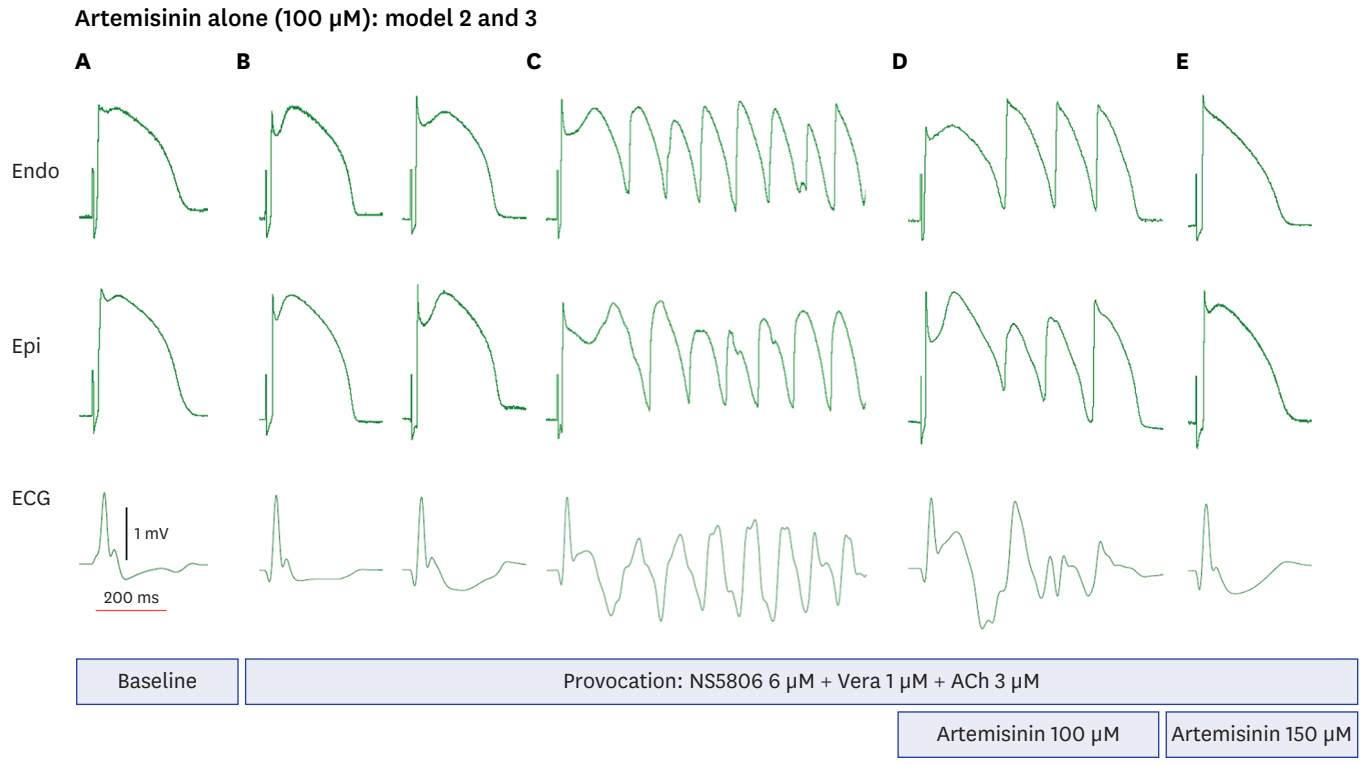

Fig. 3. AP and ECG findings of artemisinin alone (150 μM) in models 2 and 3. (**A**) Baseline AP. (**B**) Provocation agents (NS5806, Vera, and ACh) induce BrS phenotypes. The Epi AP notch becomes more prominent over time. (**C**) The provocation agents trigger PVT. (**D**) Then, 100 μM of artemisinin is infused. However, non-sustained VTA is still detected after the infusion. (**E**) An additional dose of artemisinin of up to 50 μM (total 150 μM) effectively suppresses the non-sustained VTA and restores repolarization homogeneity. After washing out artemisinin, VTA is induced again (not illustrated in this figure).
Endo = endocardium, Epi = epicardium, ECG = electrocardiogram, Vera = verapamil, ACh = acetylcholine, AP = action potential, BrS = Brugada syndrome, PVT = polymorphic ventricular tachycardia, VTA = ventricular tachyarrhythmia.

verapamil (1 μM), and NS5806 (6 μM) as provocation agents (**Table 1**, **Fig. 4**). Quinidine was added to the perfusate at the time of VTA induction at a 10 μM concentration. This prevented the loss of the AP dome and the development of phase 2 reentry, resulting in the disappearance of the J wave (**Fig. 4**). **Table 2** shows the changes in TDR, notch index, and J wave area following quinidine perfusion.

Arrhythmogenesis-suppressing effects of artemisinin combined with low-dose quinidine

Fig. 5 shows AP and pseudo-ECG recordings obtained from an RV wedge preparation under baseline conditions, following perfusion with provocation agents (**Fig. 5A and B**). In **Fig. 5B**, a significant epicardial notch, ventricular arrhythmia induction, and loss of AP dome are clearly observed. All samples (six of six) exhibited an augmented J wave, ST-segment elevation, and loss of AP dome. Significant increases in TDR, notch index, notch magnitude, and J wave area ($P < 0.001$ for all) were observed (**Table 2**). VTA was induced in all sample models (**Table 1**). When the quinidine dose was raised from 0.5 to 1, 2, and 4 μM, the VTA was suppressed at 4 μM. Therefore, we selected the low dose of 1–2 μM for further analysis. Adding low-dose quinidine (1–2 μM) suppressed PVT in two of six samples (models 9 and 10). However, PVCs and loss of AP dome persisted across all samples. An additional 100 μM of artemisinin was then perfused, which effectively suppressed PVT and restored the AP dome in all samples. Despite this, PVCs persisted in two of six samples (models 8 and 11).

https://doi.org/10.3346/jkms.2025.40.e2

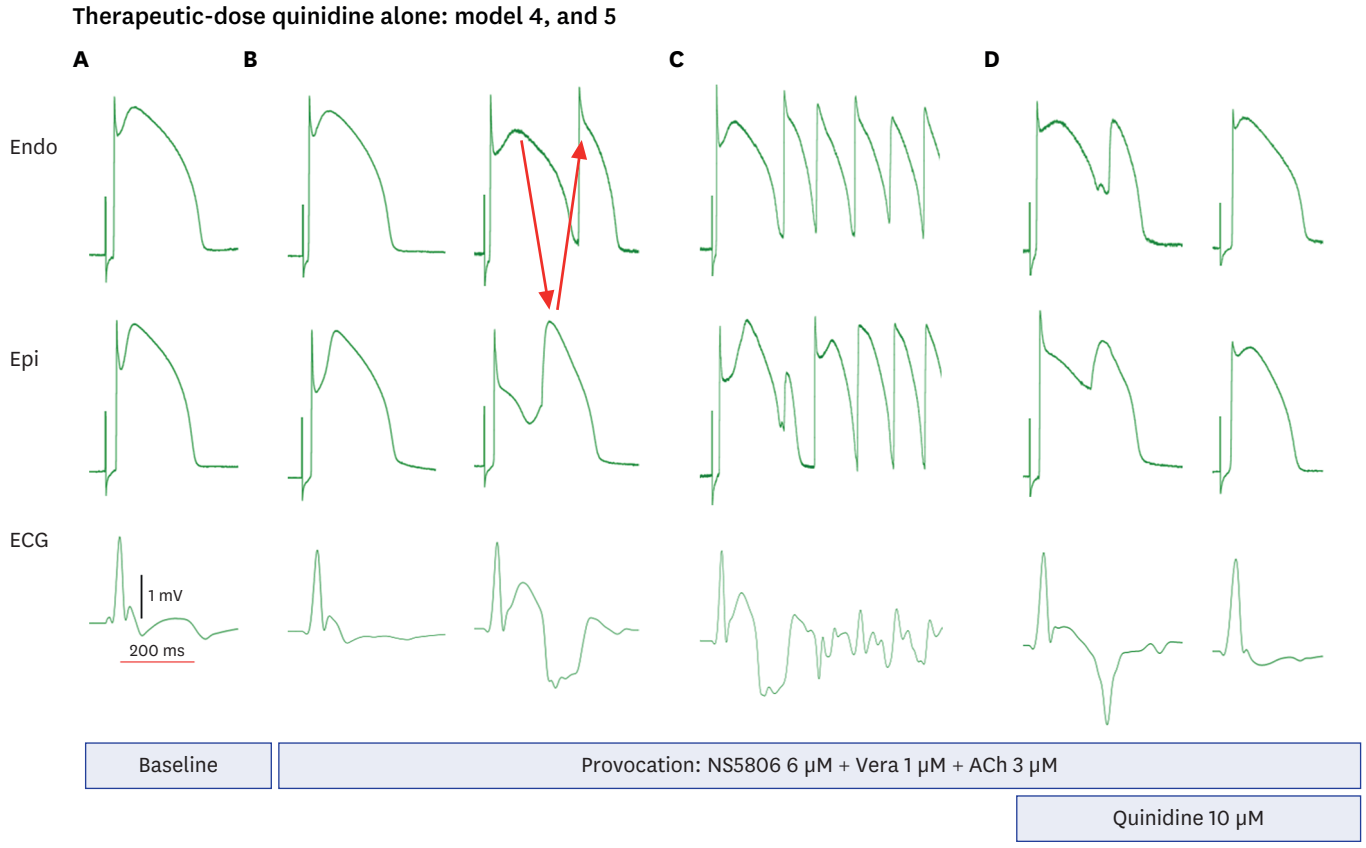

Fig. 4. AP and ECG findings of full-dose quinidine alone in models 4 and 5. (**A**) Baseline AP. (**B**) Provocation agents (NS5806, Vera, and ACh) induce BrS phenotypes. Epi AP notching is prominent, and the J wave is augmented. The provocation agents induce a phase 2 reentry (red arrow). (**C**) Eventually, PVT is induced via a phase 2 reentry. (**D**) After quinidine (10 μM) administration, the Epi AP dome is restored, and the J wave decreases. Finally, quinidine offsets the provocation agents.
Endo = endocardium, Epi = epicardium, ECG = electrocardiogram, Vera = verapamil, ACh = acetylcholine, AP = action potential, BrS = Brugada syndrome, PVT = polymorphic ventricular tachycardia.

The low-dose quinidine (1–2 μM) significantly reduced TDR (23.45 ± 0.72 ms to 20.89 ± 2.69 ms; $P < 0.001$) AP notch index (2,881.60 ± 160.57 to 1,993.04 ± 470.14; $P = 0.441$), notch magnitude (29.36 ± 1.27% to 15.48 ± 3.35%; $P < 0.001$), and J wave area (19.68 ± 1.70 mV × ms to 18.21 ± 4.89 mV × ms; $P < 0.001$) (**Table 2**, **Fig. 6**). The addition of 100 μM artemisinin significantly reduced TDR (20.89 ± 2.69 ms to 11.90 ± 1.01 ms; $P < 0.001$), AP notch index (1,993.04 ± 470.14 to 473.41 ± 116.59; $P = 0.003$), notch magnitude (15.48 ± 3.35% to 6.45 ± 1.13%; $P = 0.013$), and J wave area (18.21 ± 4.89 mV × ms to 3.31 ± 0.94 mV × ms; $P = 0.004$) (**Table 2**, **Fig. 6**). The reductions in these indices were significantly greater in artemisinin combined with low-dose quinidine than that in artemisinin or full-dose quinidine alone (**Supplementary Fig. 3**).

DISCUSSION

This study aims to examine the efficacy of combining artemisinin with low-dose quinidine in suppressing VTA in canine experimental BrS models. Artemisinin suppresses the J wave and restores the AP dome, reducing repolarization heterogeneity. This effect is attributed to its inhibition of multiple potassium channels, including the Ito, similar to the effect of quinidine. The findings also demonstrate that full-dose quinidine (≥ 5 μM) effectively

https://doi.org/10.3346/jkms.2025.40.e2

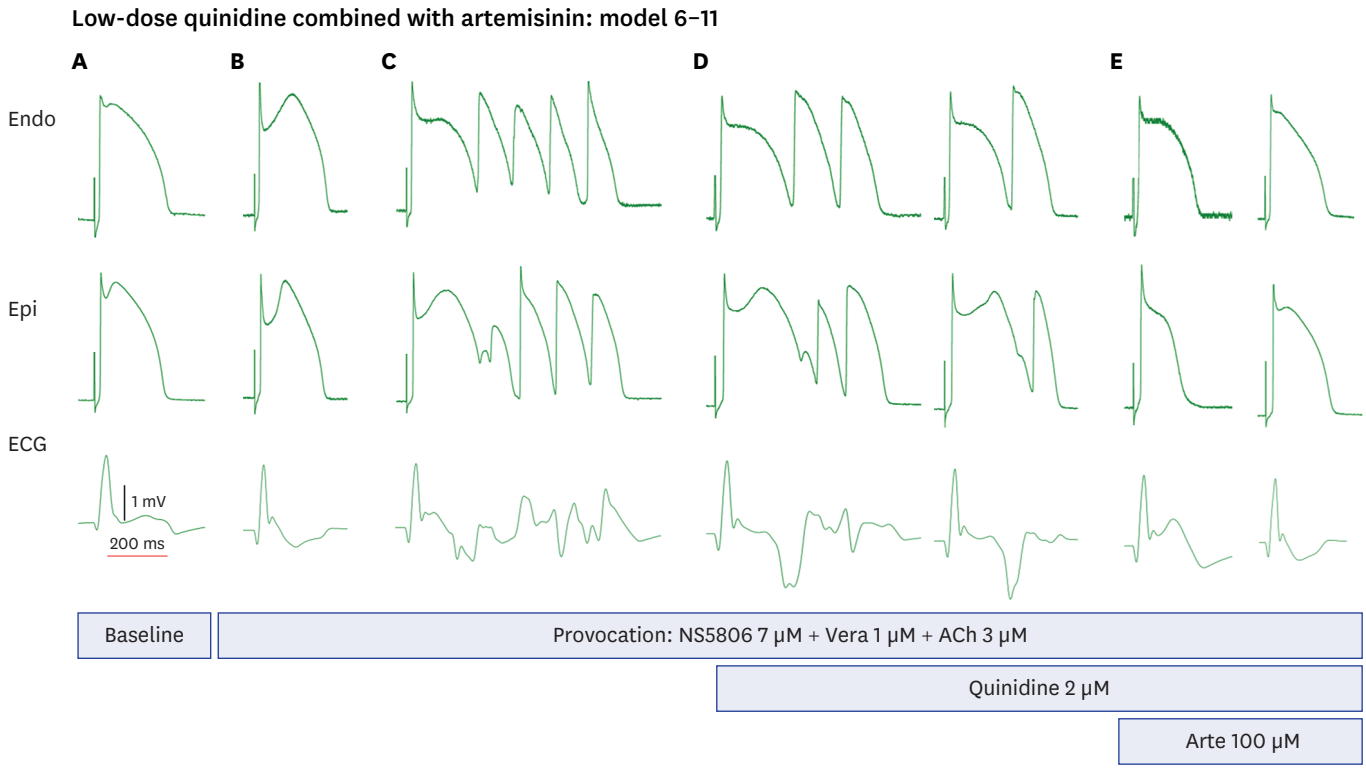

Fig. 5. AP and ECG findings of low-dose quinidine combined with artemisinin in models 6–11. (**A**) Baseline AP. (**B**) Provocation agents (NS5806, Vera, and ACh) induce BrS phenotypes. (**C**) The provocation agents induce PVT. (**D**) After the infusion of 1–2 μM quinidine, non-sustained VTA and phase 2 reentry are still detected. (**E**) The 100 μM of Artemisinin was added to perfusate, and it effectively suppresses the VTA and restores repolarization homogeneity.
Endo = endocardium, Epi = epicardium, ECG = electrocardiogram, Vera = verapamil, ACh = acetylcholine, AP = action potential, BrS = Brugada syndrome, PVT = polymorphic ventricular tachycardia, VTA = ventricular tachyarrhythmia.

suppresses VTA and restores the AP dome, while the low-dose quinidine (1–2 μM) alone did not fully suppress VTA in the BrS wedge preparation model. However, combining low-dose quinidine with artemisinin (100 μM) significantly suppressed VTA and restored the AP dome. These findings suggest that artemisinin may reduce the therapeutic dose of quinidine by further inhibiting potassium channels, including the Ito channel current. This novel finding addresses the purpose of this study.

The only proven preventive therapeutic strategy for SCD in patients with BrS is an ICD.[13,14] However, ICD is not a fundamental treatment, highlighting the need for pharmacologic strategies to suppress VTA in BrS. Therapy aims to rebalance the currents during the early phase of the epicardial AP by increasing inward currents, such as INa or ICa, and decreasing outward currents, such as Ito. Studies have explored several agents, including cilostazol, milrinone, and isoproterenol, for their potential to suppress VTA and typical BrS ECG manifestations.[24] Isoproterenol also increases ICaL channels. Higher concentrations of cilostazol directly inhibit Ito channels.[25] However, among several agents, current guidelines only recommend quinidine and cilostazol.[14] On the other hand, the guideline recommends RVOT epicardial ablation for patients experiencing recurrent ICD shocks. Nademanee et al.[26] targeted fractionated electrogram sites in the RVOT epicardium, believed to represent late potentials due to conduction abnormalities, effectively reducing VTA. Conversely, Patocskai et al.[27] show that fractionated electrograms are caused by repolarization abnormalities from an outward current shift during the early phase of the AP in epicardial ablation in an animal model.

https://doi.org/10.3346/jkms.2025.40.e2

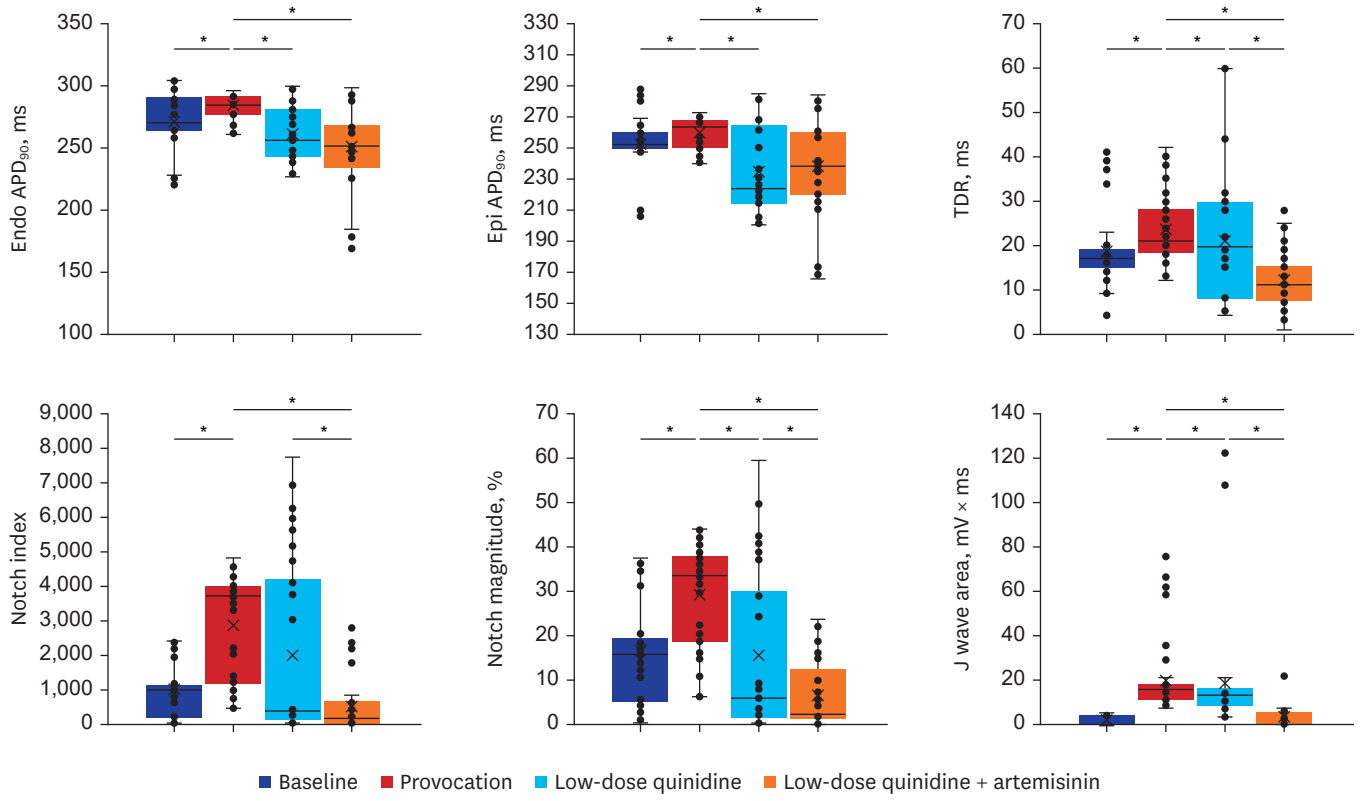

Fig. 6. Serial changes in AP parameters during provocation, low-dose quinidine, and the combination of low-dose quinidine with artemisinin. Values are presented as mean ± standard error.
Endo = endocardium, APD_{90} = action potential duration at 90% repolarization, Epi = epicardium, TDR = transmural dispersion of repolarization, AP = action potential.
*$P < 0.05$.

Quinidine is a potent Ito channel inhibitor. Previous studies show its ability to reduce repolarization heterogeneity, which decreases VTA and ICD shocks. The findings confirm its effectiveness in suppressing VTA and restoring the AP dome (**Fig. 4**). The clinically recommended dose of quinidine (900 mg to 1.5 g/day) for patients with BrS is based on electrophysiological studies with drug testing.[28] However, many patients who were prescribed quinidine discontinued treatment during follow-up owing to adverse side effects.[10] These side effects, such as diarrhea, hepatotoxicity, thrombocytopenia, and proarrhythmic effects, are dose-dependent.[11] Consequently, finding a novel agent capable of reducing the required therapeutic dose of quinidine in treating BrS would be beneficial.

Artemisinin, known for its antimalarial properties, binds to iron and breaks down its peroxide bridge, generating free radicals that damage the protein of the malaria parasite.[29] It is metabolized by CYP3A4 and CYP2B6 and also acts as a CYP3A4 inducer and TNF-α gene expression inhibitor.[30,31] Although significant side effects are rare in large clinical studies, animal studies demonstrate some side effects, such as neurotoxicity and embryotoxicity.[32] Beyond its antimalarial effects, some researchers have reported the effect of artemisinin against arrhythmias, owing to its inhibition of multiple ion channels, including IK1, Ito, and IKs channels. Yang et al.[19,20] indicate that artemisinin inhibits the Ito channels in Purkinje fibers by 84% at a 100 μM concentration, with the effect being concentration-dependent and reversible. Artemisinin also exhibits antiarrhythmic properties in BrS wedge preparation models.[21]

https://doi.org/10.3346/jkms.2025.40.e2

The mechanism by which artemisinin exerts antiarrhythmic effects on J waves and VTA may involve the suppression of potassium channels, including Ito channels. This mechanism is thought to be similar to that of other Ito channel inhibitors, such as quinidine.[9] Briefly, from the perspective of the repolarization defect theory in BrS, exposure to provocative agents leads to the loss of the AP dome in the epicardium, while the dome remains preserved in the endocardium. This creates a transmural voltage gradient, which accentuates the J wave, induces ST-segment elevation, and increases TDR. Establishing a phase 2 reentry circuit between the epicardium and endocardium is crucial to generating a vulnerable window. Ultimately, this results in the occurrence of closely coupled extrasystoles and VTA. We hypothesize that artemisinin reduces the TDR, which represents repolarization heterogeneity, by inhibiting Ito channels, thus preventing VTA. After the addition of artemisinin, AP domes were restored, VTA did not recur, and the J wave diminished in this experiment.

Artemisinin-quinidine combination successfully suppresses VTA in BrS while mitigating the adverse effects of quinidine. This is the main finding of the study. Quinidine is a well-established drug for BrS, but as mentioned in the introduction section, its side effects cause patients to stop medication. Although our previous study demonstrates that artemisinin alone (≥ 150 μM) has antiarrhythmic effects, clinical data remain lacking. Therefore, this study aims to show that combining artemisinin with clinically established quinidine could enhance its effectiveness. However, if quinidine is used at its full therapeutic dose or an adverse-effect-inducing dose, no justification exists for this combination. In this study, we evaluated the antiarrhythmic effects of quinidine by increasing the dose from 0.5 to 1, 2, and 4 μM. At 4 μM, quinidine suppressed the VTA. Thus, we selected a low dose (1–2 μM of quinidine). At this point, the low-dose quinidine should not be completely ineffective, as this would negate the need for the combination. The low-dose quinidine may appear ineffective when it is used alone in **Table 1**. However, 1–2 μM of quinidine showed significant changes in parameters, including TDR, an indicator of arrhythmogenic potential (**Table 2**). We believe that these changes were not enough to suppress VTA completely. Therefore, when artemisinin (100 μM) was added, the VTA was successfully suppressed.

Briefly, 1) The 5–10 μM of quinidine effectively inhibited Ito channels and suppressed VTA. 2) The 1–2 μM of quinidine insufficiently mitigated Ito channels, and it did not suppress VTA completely, as shown in the present study. 3) The 150 μM of artemisinin effectively inhibited Ito channels and suppressed VTA, as seen in a previous study. 4) Quinidine (1–2 μM) combined with artemisinin (100 μM) effectively inhibited Ito channels and suppressed VTA in the current study. Therefore, we believe this combination would successfully suppress VTA in BrS while reducing the adverse effects of quinidine.

In this study, we hypothesize that the combination of artemisinin further inhibits potassium currents, including Ito channels, when low-dose quinidine alone is insufficient to restore the AP dome. Additionally, it is very interesting that artemisinin also inhibits INa currents, similar to quinidine. However, no conduction delay was observed after the infusion of quinidine and artemisinin in this study. Therefore, the antiarrhythmic effect does not appear to arise from changes in depolarization properties in the BrS model induced by NS5806.

Previous studies have explored combining other agents with quinidine for BrS, including Wenxin Keli. Wenxin Keli suppresses arrhythmias by inhibiting the Ito channel, altering APs and pseudo-ECG patterns, similar to the findings in this study.[33,34] Combining Wenxin Keli with low-dose quinidine for VTA suppression in BrS models is beneficial owing to

https://doi.org/10.3346/jkms.2025.40.e2

the dose-dependent side effects of quinidine. However, the quinidine dose (5 μM) was not particularly low in that study. In previous canine BrS model studies using RV wedge preparations, quinidine of 5 μM completely inhibits VTA and restores the AP dome.[9,12] Therefore, Wenxin Keli may have been effective in conjunction with a relatively strong partner at this dose. In the present study, we evaluated a low-dose quinidine (1–2 μM) to determine if artemisinin could reduce the required dose. While low-dose quinidine (1–2 μM) alone did not completely inhibit VTA, its combination with artemisinin significantly enhanced the antiarrhythmic effect.

In this study, the artemisinin combination effectively suppressed PVT. However, PVCs persisted in two of the preparations (**Table 1**: models 8 and 11). The dose required to suppress VTA varied among preparations. Szél and Antzelevitch[35] described PVCs as a form of concealed phase 2 reentry. Considering the dose-dependent effects of artemisinin, higher concentrations may be required to fully eliminate PVCs.

The present study has some limitations. Given that these findings were obtained from experimental animal models, caution should be exercised when extrapolating them to clinical practice. Further research involving in vivo animal or clinical studies is necessary to confirm the potential application of artemisinin in BrS treatment. However, the wedge preparation model has effectively been employed to identify quinidine and cilostazol as treatments for BrS, both of which are now employed clinically. Therefore, this model is recognized for its high predictive accuracy in evaluating pharmacologic agents. The exact dosage of each drug required for suppressing VTA was not determined in this study. Although previous studies show dose-dependent actions for each drug, further investigation is needed to explore potential interactions between them.

In conclusion, this study highlights the antiarrhythmic effect of artemisinin in the BrS wedge preparation model induced via NS5806. Furthermore, it demonstrates that combining artemisinin with low-dose quinidine can enhance the antiarrhythmic effect. Given the common side effects of quinidine, artemisinin may offer a promising option to reduce the therapeutic quinidine dose for VTA suppression in BrS, potentially through additional inhibition of potassium channel, including the Ito current. However, further clinical data is required to support this hypothesis.

SUPPLEMENTARY MATERIALS

Supplementary Fig. 1

Measurement of AP. (**A**) Measurement of J wave parameters. The J wave area is calculated as mV × ms. (**B**) Measurement of AP parameters and TDR when the AP dome is maintained or lost.

Supplementary Fig. 2

AP and ECG findings in the control group wedge preparations. No significant changes are observed in the J wave and AP duration.

Supplementary Fig. 3

Decrease in notch magnitude, notch index, and J wave area is greater in Q + A than in quinidine or artemisinin alone. (**A**) Absolute values are displayed. (**B**) Relative changes are displayed, with provocation set as 100%.

https://doi.org/10.3346/jkms.2025.40.e2

REFERENCES

1. Brugada J, Campuzano O, Arbelo E, Sarquella-Brugada G, Brugada R. Present status of Brugada syndrome: JACC state-of-the-art review. *J Am Coll Cardiol* 2018;72(9):1046-59. PUBMED | CROSSREF
2. Krahn AD, Behr ER, Hamilton R, Probst V, Laksman Z, Han HC. Brugada syndrome. *JACC Clin Electrophysiol* 2022;8(3):386-405. PUBMED | CROSSREF
3. Behr ER, Ben-Haim Y, Ackerman MJ, Krahn AD, Wilde AAM. Brugada syndrome and reduced right ventricular outflow tract conduction reserve: a final common pathway? *Eur Heart J* 2021;42(11):1073-81. PUBMED | CROSSREF
4. Wilde AA, Postema PG, Di Diego JM, Viskin S, Morita H, Fish JM, et al. The pathophysiological mechanism underlying Brugada syndrome: depolarization versus repolarization. *J Mol Cell Cardiol* 2010;49(4):543-53. PUBMED | CROSSREF
5. Antzelevitch C, Yan GX, Ackerman MJ, Borggrefe M, Corrado D, Guo J, et al. J-Wave syndromes expert consensus conference report: emerging concepts and gaps in knowledge. *Heart Rhythm* 2016;13(10):e295-324. PUBMED | CROSSREF
6. Yoon N, Jeong HK, Lee KH, Park HW, Cho JG. Right ventricular longitudinal conduction delay in patients with Brugada syndrome. *J Korean Med Sci* 2021;36(11):e75. PUBMED | CROSSREF
7. Lambiase PD, Ahmed AK, Ciaccio EJ, Brugada R, Lizotte E, Chaubey S, et al. High-density substrate mapping in Brugada syndrome: combined role of conduction and repolarization heterogeneities in arrhythmogenesis. *Circulation* 2009;120(2):106-17. PUBMED | CROSSREF
8. Antzelevitch C. The Brugada syndrome: ionic basis and arrhythmia mechanisms. *J Cardiovasc Electrophysiol* 2001;12(2):268-72. PUBMED | CROSSREF
9. Yan GX, Antzelevitch C. Cellular basis for the Brugada syndrome and other mechanisms of arrhythmogenesis associated with ST-segment elevation. *Circulation* 1999;100(15):1660-6. PUBMED | CROSSREF
10. Belhassen B, Glick A, Viskin S. Efficacy of quinidine in high-risk patients with Brugada syndrome. *Circulation* 2004;110(13):1731-7. PUBMED | CROSSREF
11. Viskin S, Wilde AA, Tan HL, Antzelevitch C, Shimizu W, Belhassen B. Empiric quinidine therapy for asymptomatic Brugada syndrome: time for a prospective registry. *Heart Rhythm* 2009;6(3):401-4. PUBMED | CROSSREF
12. Gurabi Z, Koncz I, Patocskai B, Nesterenko VV, Antzelevitch C. Cellular mechanism underlying hypothermia-induced ventricular tachycardia/ventricular fibrillation in the setting of early repolarization and the protective effect of quinidine, cilostazol, and milrinone. *Circ Arrhythm Electrophysiol* 2014;7(1):134-42. PUBMED | CROSSREF
13. Al-Khatib SM, Stevenson WG, Ackerman MJ, Bryant WJ, Callans DJ, Curtis AB, et al. 2017 AHA/ACC/HRS guideline for management of patients with ventricular arrhythmias and the prevention of sudden cardiac death: a report of the American College of Cardiology/American Heart Association task force on clinical practice guidelines and the Heart Rhythm Society. *Circulation* 2018;138(13):e272-391. PUBMED | CROSSREF
14. Zeppenfeld K, Tfelt-Hansen J, de Riva M, Winkel BG, Behr ER, Blom NA, et al. 2022 ESC guidelines for the management of patients with ventricular arrhythmias and the prevention of sudden cardiac death. *Eur Heart J* 2022;43(40):3997-4126. PUBMED | CROSSREF
15. Conte G, Sieira J, Ciconte G, de Asmundis C, Chierchia GB, Baltogiannis G, et al. Implantable cardioverter-defibrillator therapy in Brugada syndrome: a 20-year single-center experience. *J Am Coll Cardiol* 2015;65(9):879-88. PUBMED | CROSSREF
16. Sacher F, Probst V, Maury P, Babuty D, Mansourati J, Komatsu Y, et al. Outcome after implantation of a cardioverter-defibrillator in patients with Brugada syndrome: a multicenter study-part 2. *Circulation* 2013;128(16):1739-47. PUBMED | CROSSREF
17. Giustetto C, Cerrato N, Dusi V, Angelini F, De Ferrari G, Gaita F. The Brugada syndrome: pharmacological therapy. *Eur Heart J Suppl* 2023;25(Suppl C):C32-7. PUBMED | CROSSREF
18. Klayman DL. Qinghaosu (artemisinin): an antimalarial drug from China. *Science* 1985;228(4703):1049-55. PUBMED | CROSSREF
19. Yang BF, Luo DL, Bao LH, Zhang YC, Wang HZ. Artemisinin blocks activating and slowly activating K+ current in guinea pig ventricular myocytes. *Zhongguo Yao Li Xue Bao* 1998;19(3):269-72. PUBMED
20. Yang BF, Li YR, Xu C, Luo DL, Li BX, Wang H, et al. Mechanisms of artemisinin antiarrhythmic action. *Zhongguo Yaolixue Yu Dulixue Zazhi* 1999;13:169-75.
21. Jeong HK, Hong SN, Yoon N, Lee KH, Park HW, Cho JG. Antiarrhythmic effect of artemisinin in an ex-vivo model of Brugada syndrome induced by NS5806. *Korean Circ J* 2023;53(4):239-50. PUBMED | CROSSREF

22. Fish JM, Welchons DR, Kim YS, Lee SH, Ho WK, Antzelevitch C. Dimethyl lithospermate B, an extract of Danshen, suppresses arrhythmogenesis associated with the Brugada syndrome. *Circulation* 2006;113(11):1393-400. PUBMED | CROSSREF

23. Di Diego JM, Sicouri S, Myles RC, Burton FL, Smith GL, Antzelevitch C. Optical and electrical recordings from isolated coronary-perfused ventricular wedge preparations. *J Mol Cell Cardiol* 2013;54:53-64. PUBMED | CROSSREF

24. Szél T, Koncz I, Antzelevitch C. Cellular mechanisms underlying the effects of milrinone and cilostazol to suppress arrhythmogenesis associated with Brugada syndrome. *Heart Rhythm* 2013;10(11):1720-7. PUBMED | CROSSREF

25. Xiao GS, Liao YH. Effect of cilostazol on transient outward potassium current in human atrial myocytes. *Zhongguo Ying Yong Sheng Li Xue Za Zhi* 2004;20(3):238-41. PUBMED | CROSSREF

26. Nademanee K, Veerakul G, Chandanamattha P, Chaothawee L, Ariyachaipanich A, Jirasirirojanakorn K, et al. Prevention of ventricular fibrillation episodes in Brugada syndrome by catheter ablation over the anterior right ventricular outflow tract epicardium. *Circulation* 2011;123(12):1270-9. PUBMED | CROSSREF

27. Patocskai B, Yoon N, Antzelevitch C. Mechanisms underlying epicardial radiofrequency ablation to suppress arrhythmogenesis in experimental models of Brugada syndrome. *JACC Clin Electrophysiol* 2017;3(4):353-63. PUBMED | CROSSREF

28. Belhassen B, Glick A, Viskin S. Excellent long-term reproducibility of the electrophysiologic efficacy of quinidine in patients with idiopathic ventricular fibrillation and Brugada syndrome. *Pacing Clin Electrophysiol* 2009;32(3):294-301. PUBMED | CROSSREF

29. Eckstein-Ludwig U, Webb RJ, Van Goethem ID, East JM, Lee AG, Kimura M, et al. Artemisinins target the SERCA of *Plasmodium falciparum*. *Nature* 2003;424(6951):957-61. PUBMED | CROSSREF

30. Abate G, Zhang L, Pucci M, Morbini G, Mac Sweeney E, Maccarinelli G, et al. Phytochemical analysis and anti-inflammatory activity of different ethanolic phyto-extracts of *Artemisia annua* L. *Biomolecules* 2021;11(7):975. PUBMED | CROSSREF

31. Xiong Z, Sun G, Zhu C, Cheng B, Zhang C, Ma Y, et al. Artemisinin, an anti-malarial agent, inhibits rat cardiac hypertrophy via inhibition of NF-κB signaling. *Eur J Pharmacol* 2010;649(1-3):277-84. PUBMED | CROSSREF

32. Efferth T, Kaina B. Toxicity of the antimalarial artemisinin and its dervatives. *Crit Rev Toxicol* 2010;40(5):405-21. PUBMED | CROSSREF

33. Tang Q. The effect of NcBe from Buchangwenxin on potassium channels in single rabbit ventricular myocytes. *Chin Physician Tribune* 2008;9:56-7.

34. Minoura Y, Panama BK, Nesterenko VV, Betzenhauser M, Barajas-Martínez H, Hu D, et al. Effect of Wenxin Keli and quinidine to suppress arrhythmogenesis in an experimental model of Brugada syndrome. *Heart Rhythm* 2013;10(7):1054-62. PUBMED | CROSSREF

35. Szél T, Antzelevitch C. Abnormal repolarization as the basis for late potentials and fractionated electrograms recorded from epicardium in experimental models of Brugada syndrome. *J Am Coll Cardiol* 2014;63(19):2037-45. PUBMED | CROSSREF